Acta Scientiae Veterinariae, 2026. 54: 2008.

RESEARCH ARTICLE
Pub. 2008

ISSN 1679-9216

Effectiveness of Polyaxial Clamp-Rod Internal Fixation Method in Distal Femoral Fractures: Experimental Study in a Sheep Model*

Nahit Saylak[1] & Semih Altan[2]

ABSTRACT

***Background*:** Distal femoral fractures remain a challenging orthopedic condition due to complex regional anatomy and limited availability of suitable implant options for stable fixation. Optimal stabilization must adhere to biological osteosynthesis principles while maintaining rigid mechanical support - particularly in periarticular fractures. The clamp-rod internal fixation (CRIF) system has previously demonstrated satisfactory clinical outcomes; however, the use of conventional cortical screws may predispose to screw loosening and compromised stability. The modified CRIF (M-CRIF) system, redesigned to incorporate polyaxial locking functionality, has the potential to enhance implant stability and improve healing quality. This study aimed to evaluate the feasibility and clinical performance of the M-CRIF implant compared with the conventional CRIF system in an experimental sheep fracture model.

***Materials, Methods & Results*:** Twelve clinically healthy adult Akkaraman crossbred sheep were randomly assigned to 2 equal groups: Group I (n = 6) treated with standard CRIF and Group II (n = 6) treated with M-CRIF. A standardized supracondylar femoral fracture was created in all subjects, followed by internal fixation according to group allocation. Postoperative monitoring included serial clinical examinations, pain assessment using facial expression and clinical scoring systems, gait and weight-bearing evaluations, vertical force plate analyses, and radiographic examinations on days 0, 3, 7, 14, 28, 45, and 60. On day 60, harvested femurs underwent histopathological assessment of fracture healing characteristics. Intraoperative reduction was achieved in all cases; however, clamp advancement over the bent rod portion was technically more demanding in Group I. Pain scores improved over time in both groups, but Group II showed faster reduction in discomfort, with significant differences observed between early and late time points ($P < 0.05$). Functional assessments revealed significantly superior gait and weight-bearing in Group II on days 28 and 45 ($P < 0.05$). Pressure mat data supported these findings, demonstrating higher peak vertical force values in Group II at the same time points ($P < 0.05$). Radiographic evaluations indicated progressive healing in both groups without significant intergroup differences; however, Group II displayed a more uniform and advanced callus formation pattern. Implant-related complications were limited to 1 case of cortical screw loosening in Group I and one postoperative soft-tissue infection in Group II, the latter resolving without affecting final healing. Histopathological findings revealed nearly complete replacement of cartilage templates by bone, abundant osteoblastic activity, and organized trabecular architecture in both groups, with slightly enhanced tissue remodeling in Group II.

***Discussion*:** The results indicate that incorporation of polyaxial locking screws into the clamp mechanism provides improved construct stability, encourages earlier weight-bearing, and contributes to more consistent functional recovery. Although radiographic outcomes alone were insufficient to discriminate between groups, multidimensional assessment methods - including force plate analysis and clinical scoring - clearly demonstrated the mechanical advantages of the M-CRIF system during the early healing phase. The reduced risk of screw-related complications further supports the superiority of this design in anatomically restricted distal femoral fractures. Considering current trends favoring systems that preserve local vascularity while providing rigid fixation, M-CRIF appears to satisfy both biological and biomechanical requirements more effectively than conventional CRIF.

Keywords: sheep, distal femur, CRIF, locking screw, osteosynthesis, experimental model.

DOI: 10.22456/1679-9216.152872

Received: 4 November 2025 Accepted: 28 January 2026 Published: 17 February 2026

*This article is based on the senior author's PhD thesis submitted to Dicle University, Turkey. [1]Department of Surgery, Faculty of Veterinary Medicine, Dicle University, Diyarbakir, Turkey. [2]Department of Surgery, Faculty of Veterinary Medicine, Dokuz Eylül University (DEU), İzmir, Turkey. CORRESPONDENCE: Nahit Saylak [nsaylak@gmail.com]. Department of Surgery, Faculty of Veterinary Medicine, University of Dicle. Diyarbakir, Turkey.

INTRODUCTION

Femoral fractures are frequently observed in companion animals because of trauma and account for approximately 33-38% of long bone fractures in cats and about 45% in dogs [12,21]. Although femoral fractures can be classified based on anatomical location, morphology, and fracture condition, the AO-Vet (Arbeitsgemeinschaft für Osteosynthes) system uses an alphanumeric scheme [5]. Anatomically, the femur is divided into proximal, diaphyseal, and distal regions (including distal physeal, supracondylar, unicondylar, bicondylar, and trochlear areas), with diaphyseal and distal fractures reported as the most common locations [21].

In the treatment of distal femoral fractures, the dense musculature enveloping the bone together with the complex regional anatomy presents significant challenges for implant placement. A comprehensive understanding of the biomechanical forces acting on the fracture site is crucial for selecting an appropriate implant and fixation technique [1,9,25].

Intramedullary pins frequently fail to provide sufficient rotational stability, and reconstruction, pearl, and J-plate systems may not offer adequate strength or anatomical conformity. Therefore, no clear consensus exists regarding the optimal fixation method for distal femoral fractures, and multiple strategies have been proposed [10,23].

The aim of this study was to provide a novel fixation option for the treatment of distal femoral fractures by redesigning the CRIF system into a lockable configuration and to evaluate the feasibility of the newly developed M-CRIF implant, which was tested for the 1st time in an experimental sheep model.

MATERIALS AND METHODS

Animals

The material of the study consisted of 12 clinically healthy, adult Akkaraman crossbred sheep with a mean age of 35 ± 3 months, used in an experimental design. Prior to the study, all animals underwent a 10-day quarantine period. Routine physical examinations were performed, and standard treatments (internal and external antiparasitic applications, *Clostridium* vaccination) were administered. Three days before the experiment, the wool of all sheep was clipped, ectoparasitic solutions were applied, and the animals were divided into 2 groups based on body weight.

The average body weight was recorded as 35.5 ± 1.52 kg for Group I (n = 6; treated with standard CRIF implants) and 34.5 ± 1.52 kg for Group II (n = 6; treated with modified CRIF implants).

Implant design and features

The CRIF implant system used in this study consists of a rod-clamp-screw combination that operates on the principle of an internalized external fixator. In the specially designed system, the rods are round and straight, made of grade 5 titanium, with a diameter of 5 mm and a length of 14 ± 4 cm. A rod bender was used to adjust the rods according to the anatomical structure of the femur (Orthocat)[1].

In the modified CRIF system, threads were added to the clamp section where the screw is placed, enabling the use of locking screws. This modification allowed for the application of cortical screws of various lengths and diameters, both straight and locking. In the standard CRIF group, the clamps were fixed onto the rod and designed to accommodate non-locking, straight cortical screws. In the modified CRIF (M-CRIF) group, the clamps were designed with a polyaxial structure that permitted the screw head to lock into the clamp housing, allowing for the insertion of spongious screws at various angles in the distal fragment to accommodate the spongious bone structure (Figure 1).

Preoperative preparation and anesthesia

Prior to surgery, subjects were transferred to the anesthesia preparation room and an appropriate catheter was placed in the cephalic vein of the forelimb. For antibiotic prophylaxis, cefazolin sodium[2] [Cezol® - 20-22 mg/kg, IV] before the procedure and repeated if the operation exceeded 1 h. a standardized anesthesia protocol was followed for all cases. Preanesthesia was achieved with butorphanol tartrate[3] [0.2 mg/kg, IM] and medetomidine HCl[4] [Domitor® - 40 mcg/kg, IM]. Anesthesia was induced by slow intravenous infusion of propofol[5] [Pofol® - 5 mg/kg, IV], followed by placement of an appropriately sized endotracheal tube (8-9 mm). Maintenance of anesthesia was provided with 1-3% isoflurane[6] [Forane Liquid®], in 100% oxygen at a flow rate of 3 L/min.

Surgical procedure and creation of the experimental fracture line

Following preoperative preparation and induction of anesthesia, the stifle joint was identified by

palpating the patella and the lateral trochlear ridge. A craniolateral skin incision was made from the greater trochanter to the patella along the femoral midline. The subcutaneous tissue and superficial fascia were incised, and blunt dissection was used to retract the subcutaneous tissues. The fascia lata was incised along the cranial margin of the biceps femoris, which was then retracted caudally to expose the femoral diaphysis. The vastus lateralis muscle was retracted by incising the fascial aponeurotic septum and releasing the loose fascia between the bone and muscle, allowing exposure of the femoral diaphysis. The incision was extended distally toward the stifle joint, curving along the lateral margin of the patella and patellar ligament.

A sterile catheter was introduced into the stifle joint to guide the osteotomy site and facilitate implant placement. After exposing the osteotomy line, surrounding muscles were retracted. An experimental supracondylar fracture was created approximately 0.5 cm proximal to the femoral metaphysis using a Gigli wire saw, with continuous irrigation using sterile saline to prevent thermal injury and remove bone debris (Figure 2). This approach aligns with established protocols for creating standardized experimental fractures in large animal models, emphasizing precision and reproducibility [13].

Fracture reduction and fixation techniques

In Group I, anatomical reduction was achieved, and a pre-bent rod was positioned along the femur. Clamps were placed on both proximal and distal fragments, and non-locking cortical screws were inserted after drilling and depth measurement. In Group II, polyaxial clamps and locking screws were used for the M-CRIF system on the distal fragment. Radiographic evaluation confirmed reduction and implant positioning before wound closure.

Postoperative management

After implant placement, anesthesia depth was reduced, and animals were extubated upon return of the swallowing reflex. Postoperative monitoring continued until sternal recumbency was achieved, after which animals were returned to their paddocks. In the postoperative period, all cases received 7.0 mg/kg amoxicillin and 1.5 mg/kg clavulanic acid[7] [Synulox® - SC for 3 days]. For analgesia, meloxicam[8] [Metacam - 20 mg/mL, single SC dose of 0.5 mg/kg/day], with additional doses given if deemed necessary. No limb suspension, bandaging, or any other supportive or restrictive interventions were applied postoperatively. Following recovery from anesthesia, the animals resumed their routine daily activities.

All postoperative assessments were performed by the same investigator to minimize variability. Pain scoring was conducted at 2, 4, 6, 24, 48, and 72 h postoperatively using the facial expression assessment scale developed by McLennan *et al*. [15], evaluated independently by 3 observers. To enhance reliability, a clinical pain scoring system commonly used in ruminants was also applied by the same 3 observers, and all data were recorded [15,28]. The initial clinical examination was performed on day 0 (after recovery from anesthesia) and subsequently on days 3, 7, 14, 28, 45, and 60. The surgical wound was inspected daily until suture removal on day 10. For clinical assessment of fracture healing, the 6-point gait and weight-bearing scoring system described by Öztaş and Avki [17] was used on days 0, 3, 7, 14, 28, 45, and 60, with findings scored from 1 to 6. Radiographic evaluations of the affected limb (craniocaudal and mediolateral views) were performed on days 0, 7, 14, 28, 45, and 60, and scored from 1 to 4 according to the radiological scoring system [17]. Vertical force plate analyses were conducted on days 0, 3, 7, 14, 28, 45, and 60 by the same personnel at consistent times. During measurements, the sheep's eyes were covered with adhesive bandages, and 3 measurements per limb were averaged. On day 60, the left femurs were harvested, fixed in 10% formalin, decalcified with EDTA, embedded in paraffin, sectioned at 5 μm, stained with Masson Trichrome, and histopathologically evaluated for new bone formation, collagen fibers, trabecular structure, cellular response, and vascularization.

Statistical analysis

All statistical analyses were conducted using IBM SPSS Statistics software, version 25.09 (IBM Corp., Armonk, NY, USA). All data obtained from the study were 1st subjected to normality testing. For pairwise comparisons, the Student's t-test was used for normally distributed data, while the Mann-Whitney U test was applied for non-normally distributed data. For comparisons among multiple groups, ANOVA or Kruskal-Wallis tests were conducted according to the distribution of the data. Bonferroni correction was applied for multiple comparisons. The mean values of relevant parameters were presented as mean ± standard deviation in tables. A P-value of < 0.05 was considered statistically significant

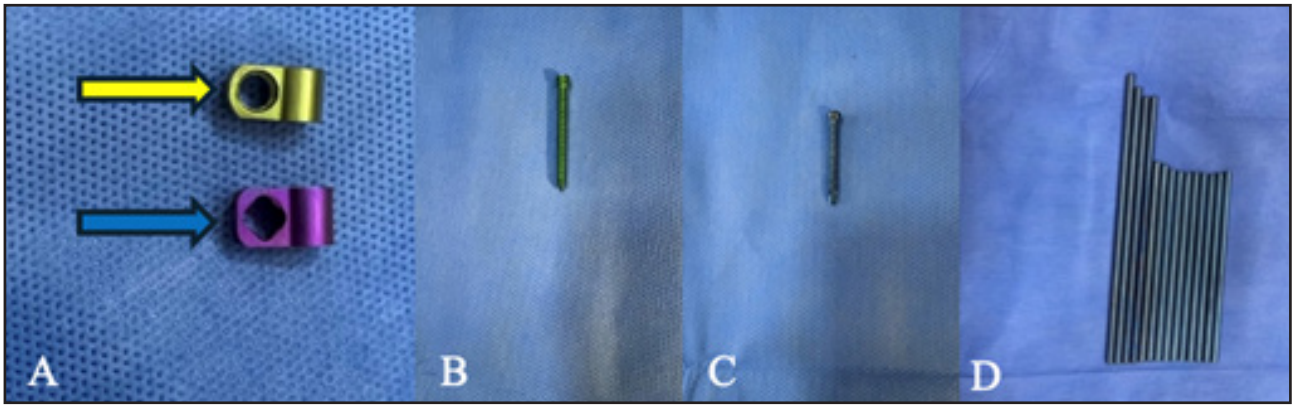


Figure 1. Orthopedic implant materials used in the study. A- Straight clamp (yellow arrow), lockable clamp (blue arrow). B- Locking screw. C- Non-locking screw. D- Rods of different lengths.

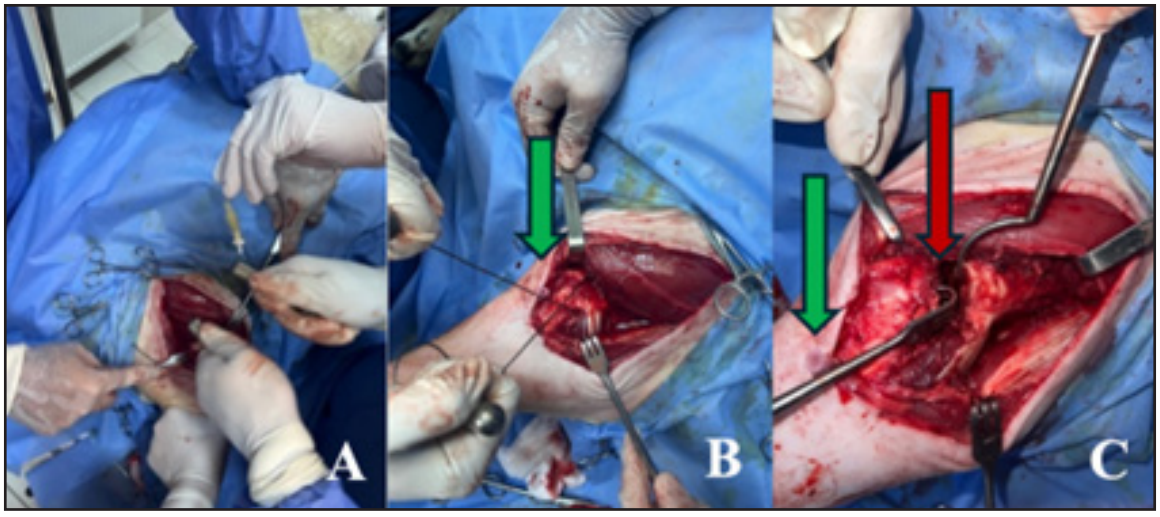


Figure 2. Creation of the experimental fracture line. A- Passage of the Gigli wire beneath the femur. B- Osteotomy of the femur at the supracondylar region using the Gigli wire (the pink catheter shown with the green arrow was inserted into the stifle joint and used as a guide). C- Supracondylar fracture fragment in the femur (red arrow).

RESULTS

During the operation, adjustment of the rods to the femoral anatomy was easy, feasible, and rapid. However, placement of the clamps onto the rod was challenging and time-consuming due to the bent segment of the rod. No difficulties were encountered during clamp placement from the distal and proximal ends of the rod. Following the creation of the experimental supracondylar fracture line, achieving anatomical reduction proved to be demanding.

In intra-group clinical pain assessments, a statistically significant difference was observed between day 1 and both day 3 and day 5 values ($P < 0.05$).

When evaluating changes in the facial pain scale over time within the groups, Group I demonstrated statistically significant differences between the 2nd h and both the 6th and 72nd h ($P < 0.05$). Additionally, a significant difference was found between the 6th and 24th h ($P < 0.05$). In Group II, significant differences were identified between the 6th h and both the 24th and 72nd h ($P < 0.05$), as well as between the 24th and 72nd h ($P < 0.05$; Figure 3).

A statistically significant difference was observed between the groups in the clinical gait score on postoperative days 28 and 45 ($P < 0.05$). When data were compared over time within Group I, statistically significant differences were found between days 3 and 14 and day 60 ($P < 0.05$; Table 1).

Significant temporal changes in radiological parameters within patient groups are frequently observed in postoperative and longitudinal imaging studies. Both Group I (GI) and Group II (GII) showed

statistically significant differences in radiological data between early (days 7 and 14) and later time points (days 28, 45, and 60), indicating measurable progression or healing over time ($P < 0.05$; Figure 4; Table 2).

Pressure analysis data obtained from the pressure band during postoperative follow-up revealed a statistically significant difference between the groups on postoperative days 28 and 45 ($P < 0.05$; Table 3).

In the within-group comparisons across different time points, both in Group I (GI) and Group II (GII), statistically significant differences were observed between days 3 and 14, 28, 45, and 60; between days 7 and 14, 28, 45, and 60; between days 14 and 28, 45, and 60; between days 28 and 45 and 60; and between days 45 and 60 ($P < 0.05$).

Both interventions demonstrated that femoral fracture repair was characterized by progressive remodeling at the endochondral ossification and healing interface. The findings were similar in both groups. Advanced bone remodeling was observed at the fracture site in both compact and trabecular bone, with the formation of bone lamellae and a high density of osteoblasts and osteocytes in remodeling regions. Inflammatory cells were absent in the healed areas, indicating resolution of inflammation. Notably, new bone tissue formed from the periphery inward in compact bone, with osteocytes and osteoblasts localized in these newly formed regions. Lacunae containing osteocytes were present in the healing bone, and mature bone tissue exhibited Haversian and Volkmann canals. In both groups, cartilage templates at the fracture interface were completely replaced by bone, while thickened collagen fibers persisted toward the medullary region, forming an interwoven network (Figure 5).

Table 1. Clinical Gait Scoring Data (Mean ± standard deviation).

Time	3. day	7. day	14. day	28. day	45. day	60. day	*P*
GI	3.83 ± 0.4^{a}	4.50 ± 0.5^{ab}	4.16 ± 0.40^{a}	4.66 ± 0.51^{ab}	4.83 ± 0.40^{ab}	5.50 ± 0.54^{b}	$P < 0.05$
GII	4.66 ± 0.81^{a}	4.66 ± 0.81^{a}	5.83 ± 0.40^{a}	$5.83 \pm 0.40^{a*}$	$5.83 \pm 0.40^{a*}$	5.83 ± 0.40^{a}	$P < 0.05$
	$P = 0.093$	$P = 0.810$	$P = 0.093$	$P = 0.009$	$P = 0.009$	$P = 0.394$	

a-bDifferent superscript letters within a row indicate statistically significant differences ($P < 0.05$). *Different superscript letters within a column indicate statistically significant differences ($P < 0.05$).

Table 2. Statistical Data of Radiographic Findings on Postoperative Control Days (Mean ± Standard Deviation).

Time	7. day	14. day	28. day	45. day	60. day	*P*
GI	1.00 ± 0.00^{a}	1.33 ± 051^{a}	2.50 ± 0.54^{b}	3.00 ± 0.63^{b}	3.16 ± 0.75^{b}	$P < 0.05$
GII	1.00 ± 0.00^{a}	1.50 ± 054^{a}	3.16 ± 0.75^{b}	3.66 ± 0.51^{b}	3.83 ± 0.40^{b}	$P < 0.05$
	$P = 1$	$P = 0.699$	$P = 0.180$	$P = 0.132$	$P = 0.132$	

a-bDifferent superscript letters within a row indicate statistically significant differences ($P < 0.05$). *Different superscript letters within a column indicate statistically significant differences ($P < 0.05$).

Table 3. Statistical data of pressure analysis from the pressure band system (Mean ± Standard Deviation).

Time	3. day	7. day	14. day	28. day	45. day	60. day	*P*
GI	6.00 ± 0.89^{a}	6.66 ± 0.81^{a}	9.16 ± 1.16^{b}	13.66 ± 1.63^{c}	17.66 ± 0.81^{d}	22.16 ± 0.75^{e}	$P < 0.05$
GII	6.00 ± 0.89^{a}	6.66 ± 0.81^{a}	8.83 ± 1.72^{b}	16.00 ± 0.89^{c}	19.50 ± 0.54^{d}	22.66 ± 1.03^{e}	$P < 0.05$
	$P = 1$	$P = 0.818$	$P = 0.937$	$P = 0.026$	$P = 0.004$	$P = 0.394$	

a-bDifferent superscript letters within a row indicate statistically significant differences ($P < 0.05$). *Different superscript letters within a column indicate statistically significant differences ($P < 0.05$).

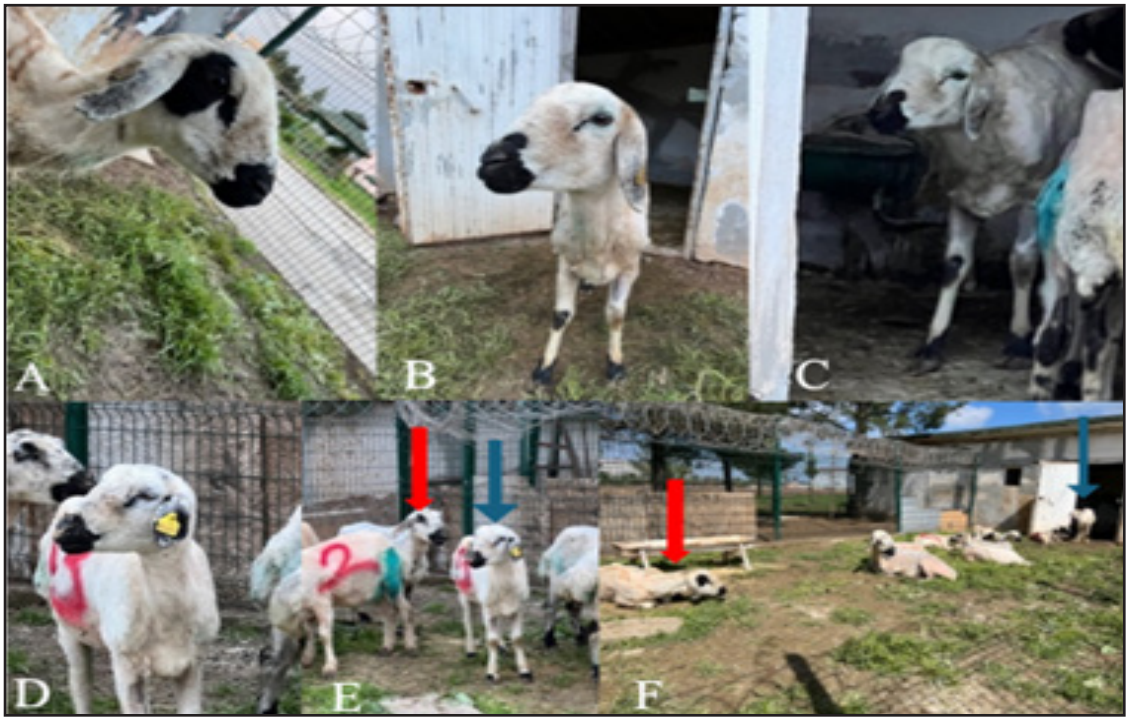


Figure 3. Evaluation of facial and clinical pain scales (Red arrow: M-CRIF Case 3; Blue arrow: CRIF Case 2). A- Tension in the masseter muscles. B- Abnormal clinical posture and a narrowed orbital angle. C- Tensed masseter muscles, hunched posture, and narrowed nasal angle. D- Tension in the masseter muscles, narrowed orbital angle, and shortened appearance of the mandible. E- Contracted, pale, and lethargic appearance while at rest. F- Clinically abnormal behavior, isolation from the flock, and absence of rumination during rest.

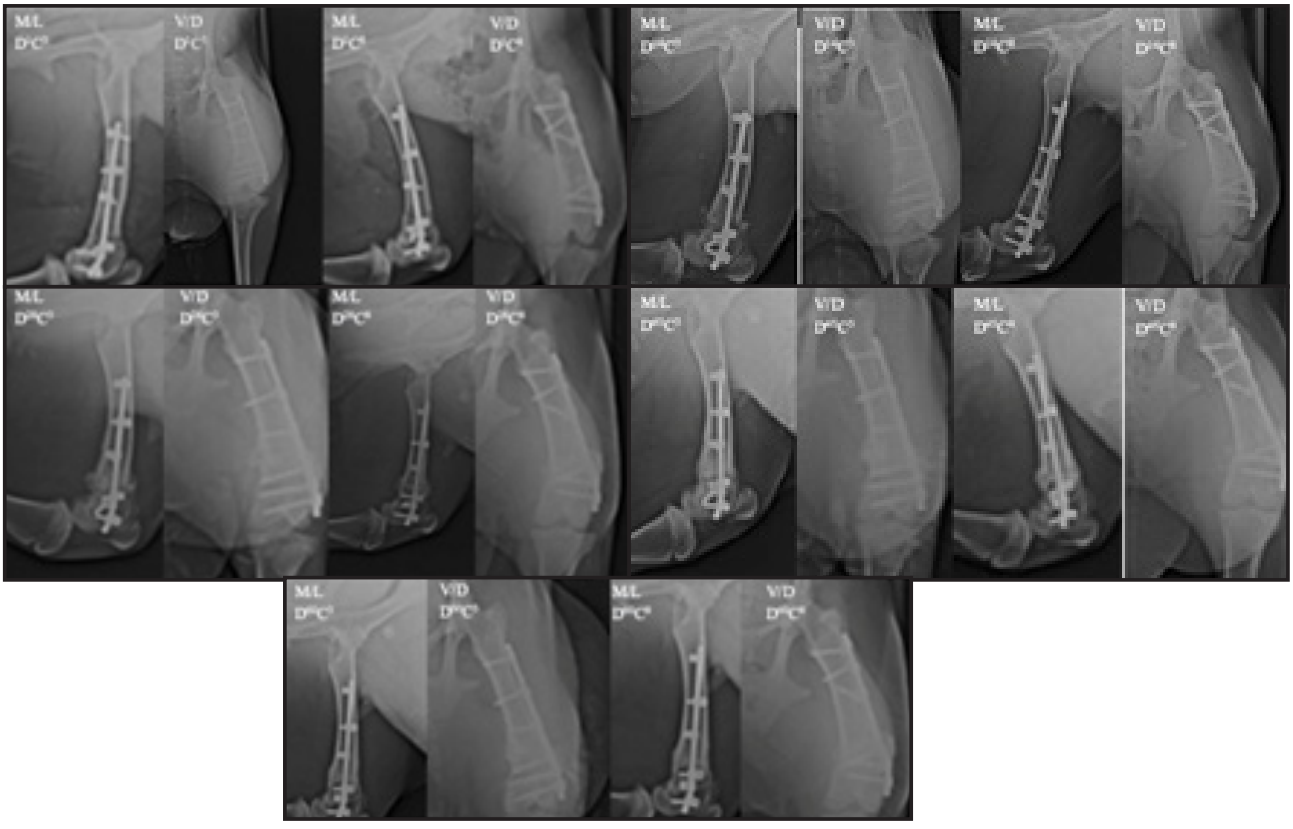


Figure 4. Representative radiographs of certain cases obtained during the course of the study. The number in the upper right corner of the letter 'D' indicates the day, whereas the number in the upper right corner of the letter 'C' represents the case.

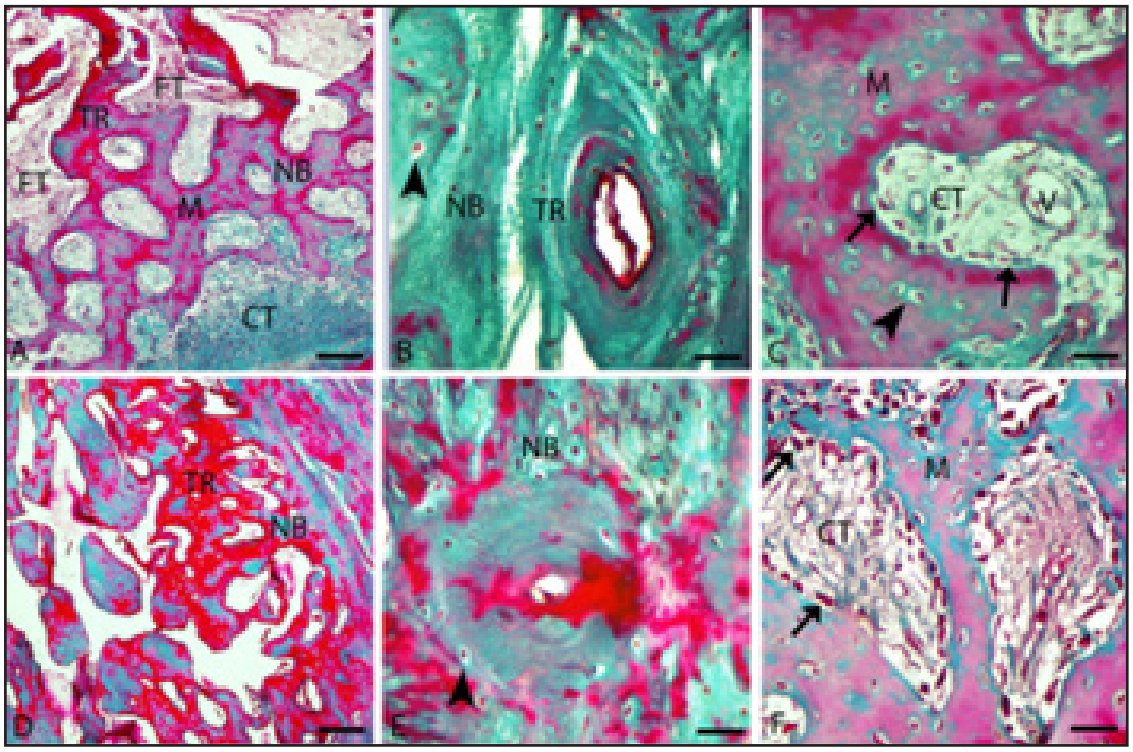


Figure 5. The appearance of bone remodeling in histologic sections of bone tissue treated with CRIF (A-C) and M-CRIF (D-F) techniques. (A &D), the new bone tissue (NB) formed in both techniques and the structure of the trabecular structures (TR) and bone matrix (M), new bone (NB) formation extending toward the center of the original surgical defect and cavities in newly formed bone tissue, and new bone (NB) remodeling in the region of bone line (BL) that was preserved. (FT) fibrotic tissue consisting of fine collagen strands deep within the bone healing zone. (B & E) osteoid structure and appearance of bone lamellae in newly formed bones. (C & F), presence of osteocytes (arrowhead) and osteoblasts (arrow) in newly formed bone tissue. Mallory's trichrome stain. [Scale bars: (A & D)=100 µm / (B, C, E & F)=25 µm].

DISCUSSION

This study aimed to evaluate the effects of a modified clamp system derived from the conventional Clamp-Rod Internal Fixation (CRIF, VetFix) design developed by the AO-Vet Orthopedic Development Institute, in which locked polyaxial functionality was incorporated into the clamps, and to assess its influence on fracture healing in an experimental sheep model. The classical CRIF system enables longitudinal rod placement contoured to the bone anatomy, with clamps and cortical screws positioned approximately perpendicular to the bone surface, providing fixation with limited implant–bone contact [27]. In the modified system, grooves were added to the clamp screw housings to allow locking, with the expectation of enhanced construct stability.

Large animal models are considered essential for the preclinical evaluation of orthopedic implants, as they permit assessment under load-bearing conditions that better reflect clinical practice. Sheep are widely accepted for orthopedic research due to their body size, bone geometry, and physiological capacity for bone healing and remodeling [4,13,14,18]. However, because sheep tend to mask pain as a prey species, pain assessment requires careful and objective evaluation [2,28]. In the present study, pain management was standardized and assessed using both facial expression scoring and a clinical pain scale. Except for one animal in each group, no relevant abnormalities were detected, and effective pain control was confirmed throughout the follow-up period, indicating that the anesthetic and analgesic protocols were appropriate [15].

Ruminal tympany represents a common anesthetic complication in sheep and can be minimized through appropriate fasting, orogastric tube placement, and right lateral recumbency [13]. In this study, withholding feed for 24 h and water for 4 h, together with standardized positioning, facilitated anesthetic management. Apart from two transient apnea episodes following propofol administration, no anesthesia-related complications were observed.

The CRIF system is generally regarded as compatible with the principles of biological osteosynthesis, as it minimizes periosteal disruption and preserves regional blood supply [1,27].

Its application is therefore considered suitable for anatomically challenging regions such as the distal femur. Nevertheless, the number of studies evaluating CRIF, particularly in large animal models, remains limited. Zahn and Matis [10] reported an overall success rate of 89% in dogs and cats, while noting technical difficulties related to clamp advancement and rod contouring. In the present study, similar challenges were encountered during clamp advancement over contoured rod segments. However, introducing clamps from the distal end of the rod proved feasible, and no rod notching was observed, possibly due to the use of titanium alloy rods rather than stainless steel.

Complications associated with CRIF constructs have previously been reported, including rod bending, axial collapse, rotational displacement, delayed union, and screw loosening [6,23]. In the current study, one complication occurred in each group: clamp loosening due to cortical screw pull-out in Group I and delayed healing associated with local infection in Group II. The former finding is consistent with previous reports indicating a higher risk of loosening with non-locking screws [7]. The absence of similar complications in Group II suggests that the use of locking screws in the modified system may confer a mechanical advantage.

Although biomechanical testing could not be performed due to ethical and logistical constraints, previous studies have shown that classical CRIF constructs exhibit lower torsional resistance than DCP or LC-DCP systems, while demonstrating comparable performance under bending loads [3,26,27]. In the modified system, locking screws engage the clamp rather than compressing the implant against the bone, thereby maintaining a fixed implant–bone distance and potentially reducing implant-related complications [26]. While DCP plates provide greater mechanical strength, their limited compatibility with biological osteosynthesis principles and technical challenges in distal femoral fractures limit direct comparison [19,27].

Functional assessment using gait scoring and pressure mat analysis revealed statistically significant differences between groups on postoperative days 28 and 45, favoring Group II. Animals treated with the modified CRIF system demonstrated earlier and more consistent weight bearing, suggesting enhanced early stability. Although radiographic scores did not differ significantly, serial imaging showed a more advanced healing pattern in Group II. Pressure mat analysis proved to be a sensitive and objective method for detecting functional differences, consistent with previous reports indicating its utility in sheep when appropriate conditioning is applied [9,12,23].

Taken together, these findings suggest that the incorporation of polyaxial locking screws into the CRIF system may improve construct stability, promote earlier functional recovery, and reduce implant-related complications, particularly in fractures involving short distal fragments. However, further biomechanical investigations and studies with larger sample sizes are required to confirm the structural advantages of the modified system [8,27].

CONCLUSIONS

In summary, both CRIF and modified CRIF constructs appear capable of accommodating the anatomical constraints of supracondylar femoral fractures in this sheep model. However, implant loosening associated with cortical screws in the classical design suggests that appropriate screw selection remains important. The polyaxial locking configuration of the modified system provided more reliable fixation and promoted more favorable early healing and functional recovery, as supported by multimodal clinical, radiographic, biomechanical surrogate and histopathological assessments. Considering the need for stable fixation while preserving local biology in fractures near the joint surface, we think that the modified clamp system may represent a promising alternative for anatomically demanding distal femoral fractures, though broader clinical investigations will be required to confirm these findings.

MANUFACTURERS

[1]Orthocat®. Orthocat Veterinary Implants. Istanbul, Turkey.

[2]Cezol®. Bilim Pharmaceuticals. Istanbul, Turkey.

[3]Butomidor®. Richter-Pharma AG. Wels, Austria.

[4]Domitor®. Zoetis. Istanbul, Turkey.

[5]Pofol®. Sandoz. Istanbul, Turkey.

[6]Forane Liquid®. Abbott Laboratories Ltd. Maidenhead, UK.

7Synulox®. Zoetis. Istanbul, Turkey.

[8]Metacam®. Boehringer Ingelheim. Istanbul, Turkey.

[9]IBM Corp. Armonk, NY, USA.

Funding. This study was financially supported by the Scientific and Technological Research Council of Türkiye (TÜBİTAK) under the 1002-A Rapid Support Program, project number 123O013. We would like to express our gratitude to the TÜBİTAK Project Office for their support.

***Ethical approval*.** This study was conducted in accordance with national and institutional animal welfare guidelines and approved by the Dicle University Local Ethics Committee (Approval No. 23/02/2022-2022/11).

***Declaration of interest*.** The authors report no conflicts of interest. The authors alone are responsible for the content and writing of the paper.

REFERENCES

1 **Beale B. 2004.** Orthopedic clinical techniques femur fracture repair. *Clinical Techniques in Small Animal Practice*.19:134-150. DOI:ORG10.1053/J.CTSAP.2004.09.006.

2 **Berset C.M., Lanker U. & Zeiter S. 2020.** Survey on sheep usage in biomedical research. *Animals*. 10: 1528. DOI. ORG/10.3390/ANİ10091528

3 **Bonin G.A., Baker S.T., Davis C.A., Bergerson C.M., Hildebrandt A.A., Hulse D.A., Kerwin S.C., Moreno M.R. & Saunders W.B. 2014.** *In vitro* biomechanical comparison of 3.5 mm LC-DCP/intramedullary rod and 5 mm clamp-rod internal fixator (CRIF)/intramedullary rod fixation in a canine femoral gap model. *Veterinary Surgery*. 43: 860-868. DOI.ORG/10.1111/J.1532-950X.2014.12130.X.

4 **Cancedda R., Giannoni P. & Mastrogiacomo M. 2007.** A tissue engineering approach to bone repair in large animal models and in clinical practice. *Biomaterials*. 28: 4240-4250. DOI:10.1016/j.biomaterials.2007.06.023.

5 **DeCamp C.E. 2015.** Femur fracture repair. In: *Brinker, Piermattei and Flo's Handbook of Small Animal Orthopedics and Fracture Repair*. 5th edn. St. Louis: Elsevier Health Sciences, pp.411-419.

6 **Delisser P., McCombe G., Trask R., Etches J., German A., Holden S., Wallace A. & Burton N. 2013.** *Ex vivo* evaluation of the biomechanical effect of varying monocortical screw numbers on a plate-rod canine femoral gap model. *Veterinary and Comparative Orthopaedics and Traumatology*. 26: 177-185. DOI: 10.3415/VCOT-12-05-0061.

7 **Field E.J., Parsons K., Etches J.A., Hamilton K. & Burton N.J. 2016.** Effect of monocortical and bicortical screw numbers on the properties of a locking plate-intramedullary rod configuration. *Veterinary and Comparative Orthopaedics and Traumatology*. 29: 459-465. DOI: 10.3415/VCOT-16-03-0040

8 **Glowacki J., Bartkowiak T., Paczos P., Mietlinski P., Zawadzki P. & Lapaj L. 2023.** Effect of screw angulation and multiple insertions on load-to-failure of polyaxial locking system. *Plos One*. 18: e0295526. DOI: 10.1371/journal.pone.0295526.

9 **Gündemir O., Alpak H., Erdikmen D.O. & Kaya D.A. 2020.** Evaluation of gait character of Akbaş and Kangal shepherd dogs by using pressure-sensitive walkway. *Turkish Journal of Veterinary & Animal Sciences*. 44: 427-434. DOI: 10.3906/vet-1907-55.

10 **Harasen G. 2002.** Fractures involving the distal extremity of the femur: Part 2 - The mature patient. *The Canadian Veterinary Journal*. 43: 131.

11 **Johnston S.A. & Tobias K.M. 2017.** *Veterinary Surgery: Small Animal Expert Consult-E-Book*. Elsevier Health Sciences.

12 **Kim J. & Breur G.J. 2008.** Temporospatial and kinetic characteristics of sheep walking on a pressure sensing walkway. *Canadian Journal of Veterinary Research*. 72: 50-55.

13 **Libardoni R.d.N., Costa D.d., Menezes F.B., Cavalli L.G., Pedrotti L.F., Kohlrausch P.R., Minto B.W. & Silva M.A.M. 2018.** Classification, fixation techniques, complications and outcomes of femur fractures in dogs and cats: 61 cases (2015-2016). *Ciência Rural*. 48. DOI: 10.1590/0103-8478cr20170730.

14 **Margolis D.S., Figueroa G., Barron Villalobos E., Smith J.L., Doane C.J., Gonzales D.A. & Szivek J.A. 2022.** A large segmental mid-diaphyseal femoral defect sheep model: Surgical technique. *Journal of Investigative Surgery*. 35: 1287-1295. DOI: 10.1080/08941939.2021.1884934.

15 **Martini L., Fini M., Giavaresi G. & Giardino R. 2001.** Sheep model in orthopedic research: A literature review. *Comparative Medicine*. 51: 292-299.

16 **McLennan K.M., Rebelo C.J., Corke M.J., Holmes M.A., Leach M.C. & Constantino-Casas F. 2016.** Development of a facial expression scale using footrot and mastitis as models of pain in sheep. *Applied Animal Behaviour Science*. 176: 19-26. DOI: 10.1016/j.applanim.2016.01.012.

17 **Moolchand M., Kachiwal A., Soomro S. & Bhutto Z. 2014.** Comparison of sedative and analgesic effects of xylazine, detomidine, and medetomidine in sheep. *Egyptian Journal of Sheep and Goats Sciences*. 9: 1-6.

18 Öztaş E. & Avki S. 2015. Evaluation of acrylic pin external fixation (APEF) system in metacarpal fractures of newborn calves: Cheap but effective? *Kafkas Üniversitesi Veteriner Fakültesi Dergisi*. 21: 453-460. DOI: 10.9775/kvfd.2014.12325.

19 Peric M., Dumic-Cule I., Grcevic D., Matijasic M., Verbanac D., Paul R., Grgurevic L., Trkulja V., Bagi C.M. & Vukicevic S. 2015. The rational use of animal models in the evaluation of novel bone regenerative therapies. *Bone*. 70: 73-86. DOI: 10.1016/j.bone.2014.07.010.

20 Perren S.M. 1991. The concept of biological plating using the limited contact-dynamic compression plate (LC-DCP). *Injury*. 22: 1-41. DOI: 10.1016/0020-1383(91)90167-9.

21 Reems M.R., Beale B.S. & Hulse D.A. 2003. Use of a plate-rod construct and principles of biological osteosynthesis for repair of diaphyseal fractures in dogs and cats: 47 cases (1994–2001). *Journal of the American Veterinary Medical Association*. 223: 330-335. DOI: 10.2460/javma.2003.223.330.

22 Roberts V.J. & Meeson R.L. 2022. Feline femoral fracture fixation: What are the options? *Journal of Feline Medicine and Surgery*. 24: 442-463. DOI: 10.1177/1098612X211033985.

23 Seebeck P., Thompson M., Parwani A., Taylor W., Schell H. & Duda G. 2005. Gait evaluation: A tool to monitor bone healing? *Clinical Biomechanics*. 20: 883-891. DOI: 10.1016/j.clinbiomech.2005.05.003.

24 Silveira F., Monotti I.C., Cronin A.M., Macdonald N.J., Rutherford S., Tiffinger K., Faux I., Rincon-Alvarez J., Kulendra E. & Tavola F. 2020. Outcome following surgical stabilization of distal diaphyseal and supracondylar femoral fractures in dogs. *The Canadian Veterinary Journal*. 61: 1073.

25 Tan C. & Johnson K. 2016. Stabilisation of periarticular fractures and osteotomies with a notched head locking T-plate. *Australian Veterinary Journal*. 94: 377-383. DOI: 10.1111/avj.12489.

26 Yayla S., Altan S., Çatalkaya E., Kanay B.E. & Saylak N. 2022. Evaluation of supracondylar femur fractures in cats: A retrospective study. *Iranian Journal of Veterinary Science and Technology*. 14: 37-41. DOI: 10.22067/ijvst.2022.77843.

27 Zahn K., Frei R., Wunderle D., Linke B., Schwieger K., Gueorguiev B., Pohler O. & Matis U. 2008. Mechanical properties of 18 different AO bone plates and the clamp-rod internal fixation system tested on a gap model construct. *Veterinary and Comparative Orthopaedics and Traumatology*. 21: 185-194. DOI: 10.3415/VCOT-07-04-0038.

28 Zahn K. & Matis U. 2004. The clamp-rod internal fixator application and results in 120 small animal fracture patients. *Veterinary and Comparative Orthopaedics and Traumatology*. 17: 110-120.

29 Zentrich E., Wassermann L., Struve B., Selke K., Buettner M., Keubler L.M., Reifenrath J., Angrisani N., Kempfert M. & Krause A. 2023. Postoperative severity assessment in sheep. *European Surgical Research*. 64: 27-36. DOI: 10.1159/000527450.

30 Zurita M. & Craig A. 2022. Feline diaphyseal fractures: Management and treatment options. *Journal of Feline Medicine and Surgery*. 24: 662-674. DOI: 10.1177/1098612X221085321.